THEORETICAL AND EXPERIMENTAL STUDIES OF Nb-BASED TUNING CIRCUITS FOR THz SIS MIXERS.

V.Yu. Belitsky[†], S.W. Jacobsson[‡], L.V. Filippenko[†], E.L. Kollberg[‡].

[†] Institute of Radio Engineering and Electronics RAS, 103907, Mokhovaja St. 11, Moscow, Russia.

[‡] Department of Microwave Technology, Chalmers University of Technology, S-412 96, Göteborg, Sweden.

Abstract

Three Nb-AlO_X-Nb SIS mixers tuned to operate in the 400-550, 550-700 and 600-750 GHz frequency bands have been investigated by modeling and experimentally by employing Fourier Transform Spectrometer (FTS) technique and mixer measurements. The mixers were of quasioptical type with spiral antennas and twin junction tuning circuits integrated onto the apex area of the antenna arms. Modeling was employed for optimizing the tuning circuits and evaluating its performance. The comprehensive model for the SIS mixer bases on Tucker-Feldman theory of quasiparticle SIS mixer and Mattis-Bardeen theory of anomalous skin-effect. Very good agreement between modeling, FTS measurements and mixer experiment results was achieved. Accuracy in prediction of the tuning band and the coupling efficiency for the tuning circuits is better or about 15% within 400-1000 GHz band.

Introduction

The SIS mixer optimum performance can be reached when the intrinsic capacitance of the SIS junction is tuned out. Different integrated on chip tuning circuits have been developed for waveguide and open structure (quasioptical) Nb-AlO_X-Nb SIS mixers for 100—820 GHz band [1-6] providing broadband low-noise operation of the receivers [7-11]. These tuning circuits mainly utilize different microstrip lines, made from Nb with SiO or SiO_2 insulator, to resonate out SIS junction capacitance.

The focus of this work is theoretical (by modeling) and experimental investigation of twin junction tuning circuit [4-6] for frequency band about 400-1000 GHz. Mattis-Bardeen theory was employed for the tuning circuit modeling. Fourier Transformer Spectrometer technique as well as mixer measurements of developed SIS mixers were used to determine tuning circuits performance, to compare experimental data and results of modeling.

At the first step of the tuning circuit development simplified free-of-loss model has been employed for evaluating of the tuning circuit behavior and its optimization [11,19]. The coupling efficiency of the spiral antenna output and the tuning circuit input was used as a quality parameter for loss-free circuitry (Fig. 1). However Fourier Transform Spectrometer (FTS) measurements of the tuning circuits [19] have shown noticeable discrepancy between tuning circuit coupling efficiency at above the gap frequency and model predicted performance. This associated with loss in Nb microstrip tuning circuitry.

Near the gap frequency of Nb material (~690 GHz for film) the Nb based microstrip lines become dispersing [12, 13] and above this frequency having increasing losses [14, 15]. Mattis–Bardeen theory [16] of skin anomalous effect describes behavior of a superconductor at these frequencies in terms of complex conductivity σ:

$$\sigma = \sigma_1 - j \cdot \sigma_2, \qquad (1)$$

where real σ_1 and imaginary σ_2 components translate directly into the normal-electron and cooper-pare currents in a superconductor. Following fundamental paper of R.L. Kautz [14] these components above can be presented in integral form:

$$\frac{\sigma_1}{\sigma_n}=\frac{2}{h\omega}\int_{\Delta}^{\infty}d\varepsilon[f(\varepsilon)-f(\varepsilon+h\omega)]\frac{\varepsilon^2+\Delta^2+h\omega\varepsilon}{(\varepsilon^2-\Delta^2)^{1/2}\left[(\varepsilon+h\omega)^2-\Delta^2\right]^{1/2}}+$$
$$+\frac{1}{h\omega}\int_{\Delta}^{h\omega-\Delta}d\varepsilon[1-2f(h\omega-\varepsilon)]\frac{h\omega\varepsilon-\Delta^2-\varepsilon^2}{(\varepsilon^2-\Delta^2)^{1/2}\left[(h\omega-\varepsilon)^2-\Delta^2\right]^{1/2}}, \quad (2)$$

and

$$\frac{\sigma_2}{\sigma_n}=\frac{1}{h\omega}\int_{\Delta(T)-h\omega,-\Delta}^{\Delta(T)}d\varepsilon[1-2f(\varepsilon+h\omega)]\frac{\varepsilon^2+\Delta^2+h\omega\varepsilon}{(\varepsilon^2-\Delta^2)^{1/2}\left[(\varepsilon+h\omega)^2-\Delta^2\right]^{1/2}}, \quad (3)$$

where T is the temperature [K], σ_n is the conductivity of a superconductor just above the critical temperature T_C, $\Delta=\Delta(T)$ is the energy gap parameter [eV], $f(\varepsilon)=1/(1+\exp(\varepsilon/kT))$ is Fermi function, ω is the angular frequency. The first integral of σ_1 represents conduction of thermally excited normal electrons, while the second integral of σ_1 introduces generation of quasiparticles by incoming radiation. The lower limit on the integral for σ_2 becomes $-\Delta$ when the frequency exceeds the gap frequency.

In [14] the relation between material parameters of a superconductor defines as below:

$$\lambda_o=\sqrt{\frac{h}{\pi\mu_o\sigma_n\Delta}} \quad (4)$$

where μ_0 is the permeability of vacuum, h is the reduced Plank's constant and λ_0 is the London penetration depth.

The specific surface impedance Z_S per unit of length of the superconducting film with thickness d is expressed as follow:

$$Z_s(\omega)=(j\omega\mu_o/\sigma)^{1/2}\coth\left[(j\omega\mu_o\sigma)^{1/2}d\right], \quad (5)$$

Microstrip line parameters, *e.g.* propagation constant γ and the characteristic impedance Z_0 with series impedance Z and admittance Y of a unit of line are:

$$\gamma=\sqrt{ZY}, \quad (6)$$

$$Z_o=\sqrt{\frac{Z}{Y}}. \quad (7)$$

Hence for particular superconducting microstrip-line with specific geometrical inductance L and capacitance C per unit length of line, Z should include Z_S (Fig. 2) that introduces additional frequency dependent inductance and surface loss. At frequencies about 600 GHz the SIS junction of μm size has to be considered as a distributed element; we assumed microstrip line model with superconducting electrodes for such junction, where the tunnel barrier is considered as insulator. Along with mentioned Z_S we add a conductance representing quasiparticle loss $G=1/R_{rf}$, (Fig. 2), where R_{rf} is input quantum impedance for signal frequency ω for unit of SIS junction line at some bias voltage U and LO power (normalized parameter $\alpha=eV_{rf}/h\omega$ with LO signal amplitude across the junction V_{rf}).

Quasi-optical SIS mixer. Tuning circuit

Three SIS mixers tuned for operation in the 400-550, 550-750 and 650-800 GHz bands have been investigated. The mixers utilize equiangular spiral antennas that were designed for operation between 230-850 GHz (inner radius of the antenna 13 μm, and outer radius 480 μm) for the 500 GHz mixer and between 350-1000 GHz (7 μm, and 315 μm, respectively) for the 600 and 700 GHz mixers. The antenna has real and frequency independent impedance 114 Ω when it is mounted onto the flat side of an extended hyperhemispherical crystal quartz lens [17]. The SIS junctions and the tuning circuit were placed at the apex of the antenna Fig. 3.

The tuning circuit [4] connects two identical (twin) SIS junctions through a microstrip transmission line, so that the reactance of the first junction is transformed to cancel the reactance of the second junction, *i.e.* the transmission line conjugates the impedance of the first junction. Then, the resulting impedance is transformed by another transmission line to match the impedance of the antenna (Fig. 4). Both junctions assumed to have identical junction areas, A, normal state resistance, R_n, as well as the same DC bias, signal and LO levels. The length of the impedance conjugator section can be chosen to compensate the reactance at one specific frequency. However, the dimensions of the two transmission lines can be adjusted to give an increased bandwidth at the expense of a ripple in the pass band (Fig. 1). The particular shape of the coupling band is a compromise between bandwidth and ripples in the pass band. The mixers for 600 and 700 GHz are scaled versions of the 500 GHz one, *i.e.* different R_nA products (20 $\Omega\mu m^2$ (J_C=10 kA/cm^2) and 25 $\Omega\mu m^2$ (J_C=8 kA/cm^2) respectively) and circuit dimensions. The realization of the detector tuning circuitry is limited by the available Nb technology. For instance, we have to use SIS junctions with $R_nA \geq 20$ $\Omega\mu m^2$ to keep the quality parameter $R_j/R_n \geq 10$, where R_j is the sub gap resistance, and the gap voltage V_g= 2.5 - 2.75 mV. Furthermore, the SiO insulation has to be thicker than ≈140 nm to prevent shorts between the microstrip and its ground plane. Due to technology limitations coupling efficiencies less than 100% for the 600 and 700 GHz mixers are the results of compromises between broadband operation and good coupling efficiencies (Fig. 1). The circuit design in more details discussed in [11,19]. Table 1 lists SIS junction parameter values as well as Table 2 lists the dimensions of the optimized tuning circuits assuming loss-free tuning circuitry.

For the twin junction tuning circuitry with loss RF power distributed from output of the antenna has to be carefully estimated for both outermost and furthermost SIS junctions; total power from the two junctions related to optimum matched power for given source impedance to evaluate quality parameter for the circuitry with loss.

Modeling of the mixer performance

Model for the Nb film

At the gap frequency Nb superconductor surface impedance dramatically changes. The gap frequency is $\omega_g = \Delta/\hbar$ and the gap energy Δ according to BCS theory depends on the temperature. The gap energy at zero temperature $\Delta(0)$ is directly related to the critical temperature of superconductor [15]. In our model we used measured the gap voltage (energy). Empirically it was found to correspond to the voltage of 10% quasiparticle current onset (Fig. 5) at given temperature (4.2 K) for the best model fitting. Expression (5) then was used to evaluate the conductivity σ_n and BCS dependence of Δ was employed to estimate $\Delta(0)$. Table 3 lists material parameters used in our modeling to describe the Nb film quality. Calculated real and imaginary components σ_1, σ_2 for the Nb films (presented in Table 3) and plotted *vs.* frequency $f=\omega/2\pi$ in Fig. 6.

Model for SIS junction

In the modeling of the SIS junction we used a piece-wise linear approximation of the SIS junction's current-voltage curve (IVC) (Fig. 5). The RF impedance of the SIS junctions was calculated for given α (LO power level) and U_{bias} (usually at the middle of the first quasiparticle step) according to Tucker-Feldman theory for quantum mixing in SIS tunnel junctions. Since the SIS junction quantum susceptance is small compared with the intrinsic junction capacitance the former was neglected in the modeling. The SIS junction capacitance was calculated according to [18] for measured R_n and estimated junction area, A, taking into account junction window over-etching.

At frequencies about 600 GHz we consider SIS junctions of μm size as distributed elements, assuming microstrip line model with superconducting electrodes for such junction, where tunnel barrier is considered as insulator. The SIS junction impedance components of 2 μm width and 1.5 μm length are presented in Figure 7 (for the junction as a lumped and distributed element). In the 600 and 700 GHz mixers SIS junction size along the microstrip was set to 1 μm to eliminate effect of distributing.

Model for Nb microstrip line

Parasitic reactance in the tuning circuit caused by steps in the strip widths and SiO insulator thicknesses have been neglected. Fig. 8 presents calculated transmission loss *vs.* frequency for transformer section lines of the tuning circuits for 500, 600 and 700 GHz mixers those have quarter-wave-length at the center frequencies of the tuning bands. At the transformer sections of the tuning circuit the condition t<<W, where t is SiO insulator thickness and W is strip width, is not valid (see Table 2). Therefore the fringing field should be taken into account correcting the microstrip impedance with about 10-15%. Fig. 9 displays a family of transmission loss curves at different ambient temperatures for the transformer section of the 600 GHz mixer. Three regions with different performance of the line could be distinguished: ***i.*** below $\approx(0.8—0.9)\omega_g$ the line is loss free; ***ii.*** in the band $\approx(0.8...0.9—1.4)\omega_g$ the line has increasing losses with a strong temperature dependence of the loss; ***iii.*** above $1.4\omega_g$ the Nb superconducting line has high transmission loss.

Model for superconducting spiral antenna

In a real mixer it is difficult to separate loss contribution from the antenna between RF optic loss, the mixer loss, *etc.* In our modeling we have tried to estimate this component of loss presenting the antenna as an equivalent microstrip line.

Spiral equiangular antenna is a traveling wave antenna, *i.e.* the antenna can be represented as a segment of transmission line with propagating electromagnetic wave along it. Spiral antenna has a continuously changing arm width. We re-presented the antenna as a microstrip line with characteristic impedance corresponding to that of the antenna onto crystal quartz hemispace (114 Ω). The strip width at distance L_l is equal to the actual dimension of the antenna arm at the same distance L_l along the arm from the apex of the antenna. Keeping the impedance of this equivalent line to be 114 Ω leads to increase of the insulator thickness for peripheral parts of the equivalent line as the antenna arm width increase. Wide-band log-spiral antenna at every frequency has active area about λ/π in diameter [20], where λ is current wavelength. However for modeling we set this dimension (related with length of the equivalent line) to be 0.4λ. It gives us about 25% overestimation of loss. Furthermore we also neglected that in the real antenna RF current rapidly decreases along the antenna arms so that loss contribution from outer parts of the spiral antenna is less than from inner. Fig. 10 shows the calculated loss *vs.* frequency for the equivalent line of the spiral antenna for 600/700 GHz mixers.

For optimized model, *i.e.* the model that provides the best fitting to measured data, no *additional* changes have been done for any samples, batches, *etc.* The input measured parameters for the model are: ***i.*** for Nb film — T_c or/and V_g at 4.2 K, λ_0; ***ii.*** for SIS junctions — R_n, V_g, A, junction dimensions; ***iii.*** for the tuning circuit — strip dimensions and layer thicknesses.

Measuring technique and results

The three mixers, *e.g.* tuned for 500, 600 and 700 GHz, have been measured using Fourier Transformer Spectrometer technique, operating as direct detectors to evaluate tuning bands and coupling efficiency (relative). In our experiments the mixers were measured in identical as possible conditions with FTS operated in frequency range 400 — 1500 GHz and with resolution about 4 GHz. No any response above ≈940 GHz were observed. The 500 GHz detector was also operated as a mixer. The 500 GHz mixer measurements have shown that cooling the mixer below 4.2 K temperature may be very advantageous for decreasing the receiver noise temperature [7]. To investigate temperature behavior of the tuning circuits and coupling efficiency all mixers were FTS tested at 4.2 and about 3.1 K temperatures. Measuring set-ups, technique in details described in [7,11,19].

Figures 11, 12 and 13 present results of FTS measurements of 500, 600 and 700 GHz mixers correspondingly at temperatures 4.2 and 3.1 K. At these figures the results of modeling for the mixers at the same temperatures are plotted as well; all data normalized. Figure 14 shows compiled measurements for all mixers with original scale and the model predicted direct detector responses. At Figure 15 the 500 GHz receiver measured noise temperatures (DSB) are plotted

with FTS data and model predicted curve for coupling efficiency *vs.* frequency (two latter curves are inverted and normalized by the receiver noise temperature at 480 GHz).

Discussion and conclusion

Our FTS and mixer measurements and theoretical investigations by modeling of the quasi-optical SIS mixers comprising superconducting spiral antenna, SIS junctions and tuning circuitry show excellent agreement of tuning bands and coupling efficiency at frequencies below the gap and very good agreement above the gap frequency for Nb material. The model of the mixer describes temperature dependence of the direct detector response correct. Although for frequencies above the gap the measurements of direct detector response show more changes with temperature than the model predicts. We believe it can be explained by presence of "critical points" in superconducting circuitry, that are beyond the model consideration, and where high DC current and dissipating power (close to SIS junction) may lead to local increasing of ambient temperature and degrading of the superconductor film. Additional cooling dramatically improves performance at these critical points.

While optimizing of the model, presentation of SIS junction as lumped element has shown better fit to the experimental data than the distributed model. We suppose that it can be explained by the fact that SIS junction introduces very sharp discontinuity for the electromagnetic wave (in its dimensions, impedance, *etc.*), so that RF current penetrates perpendicularly to the SIS junction rather then along it. Furthermore our modeling of the SIS junction with distributed line shows extremely high losses appearing at this junction line above the gap frequency. This fact explains the absence of Josephson resonance in long junctions and tuning circuitry [12,13] above the gap.

Accurate estimation of RF loss in the spiral antenna requires detail knowledge of electromagnetic field distribution in this complicated strip-slot spiral structure and complete analysis has not been done so far. Our modeling of the superconducting spiral log-periodical planar antenna, based on the equivalent line presentation, shows that RF loss in such antenna produced from superconductor at above the gap frequency not exceed ≈14% (with overestimation). This offer using pure superconducting Nb circuitry for THz SIS mixers without suggested in [21] replacing Nb film for normal metal and associated with it technological problems.

To the conclusion, the introduced modeling based on Mattis—Bardeen skin anomalous effect theory and Tucker-Feldman theory of quasiparticle mixing provides very good agreement of tuning bands and coupling efficiencies (within 15%) with mixer and FTS measurements of the twin junction tuning circuitry for the spiral antenna SIS mixers at 400 — 1000 GHz band. The model includes all important parts of the SIS open structure mixer, *i.e.* SIS junctions, microstrip tuning circuitry and spiral antenna. The experimental results and modeling show good prospects of the twin compensation circuit for frequencies up to 700 GHz.

Acknowledgments

C. Holmstedt is greatly acknowledged for very useful technical assistance. Photomasks for producing investigated mixers were made by S.L. Muratov ("Sapphire", Moscow).

This work has been supported by grants form the European Space Agency (ESA) under contracts 7898/88/NL/PB, Russian Program of Fundamental Research (contract 92-02-3484) and Russian State Scientific Program "Superconductivity" (contract No 91009), Royal Swedish Academy of Sciences, The Swedish Board for Space Activities and The Swedish National Board of Industrial and Technical Development. The Swedish Institute is acknowledged for the support of Dr. V.Yu. Belitsky during his visit at Chalmers University of Technology.

References

[1] M. J. Wengler, *"Submillimeter-Wave Detection with Superconducting Tunnel Diodes," Proc. of the IEEE*, vol. 80, pp. 1810-1826, 1992.

[2] R. Blundell, C.-Y. E. Tong, *"Submillimeter Receivers for Radio Astronomy," Proc. of the IEEE*, vol. 80, pp. 1702-1720, 1992.

[3] A. R. Kerr, S.-K. Pan, and M. J. Feldman, *"Integrated tuning elements for SIS mixers," Int. J. IR and MM Waves*, vol. 9, pp. 203-212, 1988.

[4] V. Yu. Belitsky and M. A. Tarasov, "SIS junction reactance complete compensation," *IEEE Trans. on Magnetics*, vol. MAG-27, Part. 2, pp. 2638-2641, 1991.

[5] V.Yu. Belitsky, S.W. Jacobsson, L.V. Filippenko, S.A. Kovtonjuk, V.P. Koshelets and E.L. Kollberg, *"0.5 THz SIS Receiver with Twin Junction Tuning Circuit,"* Proc. of the 4th Int. Symp. on Space Terahertz Technology, UCLA, Los Angeles, p.538, 1993.

[6] J. Zmuidzinas, H. G. LeDuc, J. A. Stern, and S. R. Cypher, *"Two-Junction Tuning Circuits for Submillimeter SIS Mixers," IEEE Trans. on MTT*, vol. 42, pp. 698-706, 1994.

[7] S. W. Jacobsson, V. Y. Belitsky, L. V. Filippenko, S. A. Kovtonjuk, V. P. Koshelets, and E. L. Kollberg, "Quasi-optical 0.5 THz receiver with twin junction tuning circuit," in proceedings of the 18'th International conference on Infrared and Millimeter Waves, pp. 267-268, Colchester, UK, 1993.

[8] P. Febvre, W.R. McGrath, P. Btelaan, B. Bumble, H.G. LeDuc, S. George and P. Feautier, *"A Low-Noise SIS Receiver Measured from 480 GHz and 650 GHz Using Nb Junctions with Integrated RF Tuning Circuits"*, Int. Journal of Infrared and Millimeter Waves, vol.15, No.6, pp.943—966, June 1994.

[9] G. de Lange, C. E. Honingh, J. J. Kuipers, H. H. A. Schaeffer, R. A. Panhuyzen, T. M. Klapwijk, H. van de Stadt, and M. M. W. M. de Graauw, "Heterodyne mixing with Nb tunnel junctions above the gap frequency," *Appl. Phys. Lett.,*, vol. 64, pp. 3039-3041, 1994.

[10] J. Zmuidzinas, N.G. Urgas, D. Miller, M. Gaidis, H. G. LeDuc, J.A. Stern, *"Low-Noise Slot Antenna SIS Mixer"*, submitted to IEEE Trans. on Applied Superconductivity.

[11] V.Yu. Belitsky, S.W. Jacobsson, L.V. Filippenko, E.L. Kollberg, *"Broad band Twin junction tuning circuit for submillimeter SIS mixers,"* in preparation.

[12] G. S. Lee and A. T. Barfknecht, "Geometrical and Material Dispersion in Josephson Transmission Lines," *IEEE Trans. on Appl. Superconductivity*, vol. 2, pp. 67-72, 1992.

[13] H. H. S. Javadi, W. R. McGrath, B. Bumble, and H. G. LeDuc, "Onset of Dispersion in Nb Microstrip Transmission Lines," in proceedings of the III Int. Symp. on Space Terahertz Technology, pp. 362-381, Univ. Of Michigan, Ann Arbor, USA, 1992.

[14] R. L. Kautz, "Picosecond pulses on superconducting striplines," *J. Appl. Phys*, vol. 49, pp. 308-314, 1978.

[15] R. Pöpel, "Surface impedance and reflectivity of superconductors," *J. Appl. Phys*, vol. 66, pp. 5950-5957, 1989.

[16] D.C. Mattis and J. Bardeen, Phys. Rev. 111, p.412, 1958

[17] T. G. Büttgenbach, H. G. LeDuc, P. G. Maker, and T. G. Phillips, "A Fixed Tuned Broadband Matching Structure for Submillimeter SIS Receivers," *IEEE Trans. on Appl. Supercond*, vol. 2, pp. 165-175, 1992.

[18] V. Y. Belitsky, S. W. Jacobsson, S. A. Kovtonjuk, E. L. Kollberg, and A. B. Ermakov, "100 GHz Mixer with Vertically Integrated (stacked) SIS Junction Array," *Int. J. of Infrared and Millimeter Waves*, vol. 14, pp. 949-957, 1993.

[19] V. Y. Belitsky, S. W. Jacobsson, L. V. Filippenko and E. L. Kollberg, "Fourier transform spectrometer studies (300 - 1000 GHz)of Nb-based quasi-optical SIS detectors," *Accepted for publication in IEEE Trans. on Applied Superconductivity,* Dec. 1994

[20] G.T. Markov, D.M. Sazonov: *Antennas* , Power Publisher (in Russian), Moscow 1975.

[21] G. de Lange, Ph.D. thesis: *Quantum limited heterodyne detection of 400-840 GHz radiation with superconducting Nb tunnel junctions*: Department of Physics, Rijksuniversiteit Groningen, The Netherlands, 1994.

Tables

Table 1

Parameter:	500 GHz mixer	600 / 700 GHz mixers
Normal state resistance R_n (two junctions in parallel) [Ω]	6	5
Junction area [μm^2]	4	2
Leakage resistance R_n (two junctions in parallel) [Ω]	60	50
Gap voltage [mV]	2.5 – 2.7	2.7 – 2.8
Gap width [mV]	10% of V_g	10% of V_g
Critical current density [kA/cm^2] / junction capacitance [pF]	8 / 0.38	10 / 0.2

Table 2

Dimensions [μm]	500 GHz mixer		600 / 700 GHz mixers	
	Conjugator	Transformer	Conjugator	Transformer
Length	12	56	6 / 4.5	41 / 37
Width	8	3	3	2.5
Top electrode thickness	0.35	0.35	0.4	0.4
SiO insulator thickness	0.15	0.3	0.33	0.33
Ground electrode thickness	0.2	0.2	0.2	0.2

Table 3

Nb material critical temperature T [K]	8.1	8.4	9.0
Normal state conductivity $\sigma_n x 10^{-7}$ [$\Omega^{-1}m^{-1}$]	1.74	1.67	1.57
Gap voltage [mV] at temperatures T = 0 K/4.2 K	2.65/2.53	2.75/2.65	2.95/2.85
Penetration depth λ_O [μm]	0.86	0.86	0.86

Figures

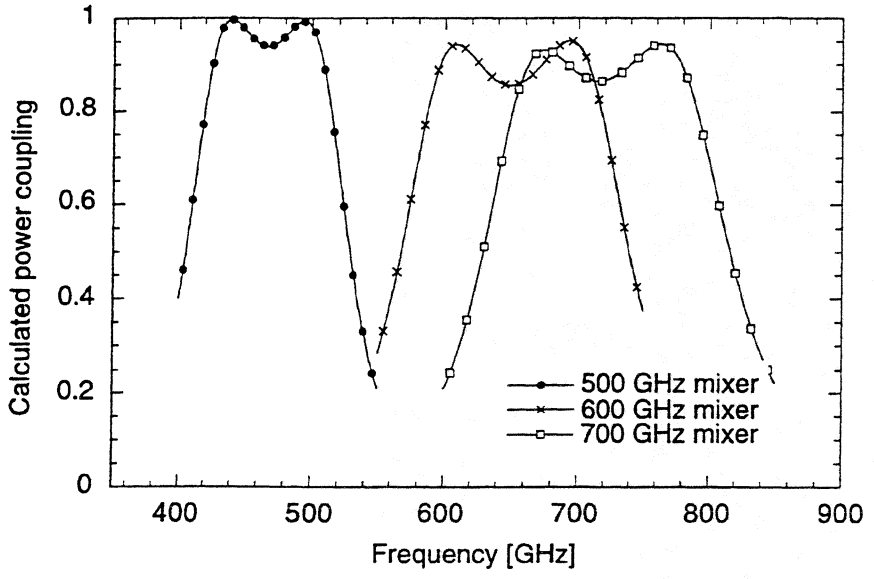

Figure 1 *Modeled performance of the investigated mixers. Modeling was made assuming loss-free microstrip lines. The fabricated 600 and 700 GHz samples were measured to have their best coupling located at higher frequencies than those of the modeled circuits. The reason was found to be improper thickness of the SiO layer in the microstrip transmission line between the junctions.*

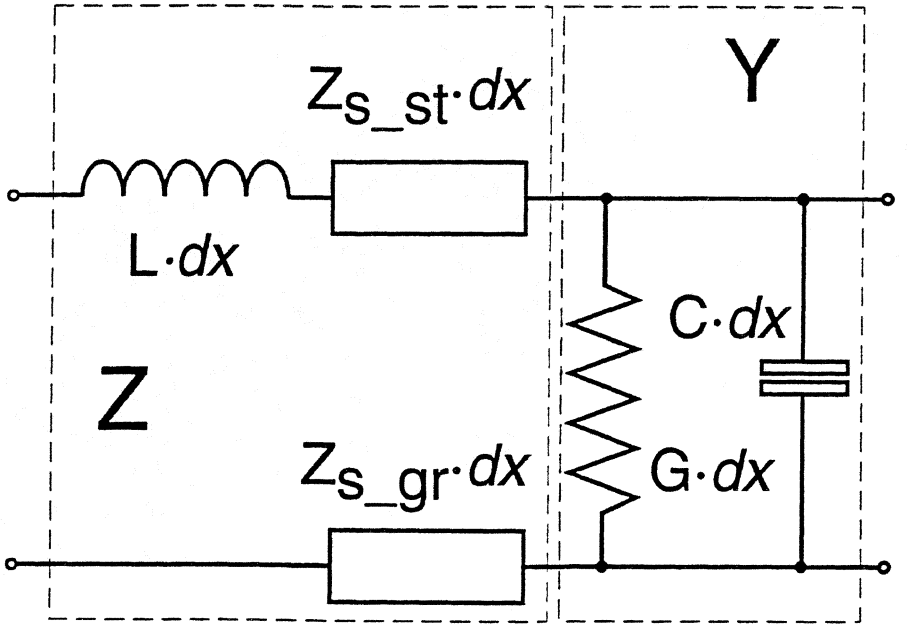

Figure 2 *Circuit diagram for cell of superconducting microstrip line. L, C are specific geometrical inductance and capacitance per unit of length; Z_{s_st}, Z_{s_gr} are surface resistance of microstrip and ground electrodes correspondingly defined according to (5); $G=1/R_{rf}$ is quasiparticle quantum non-linear conductance of a unit of SIS junction line.*

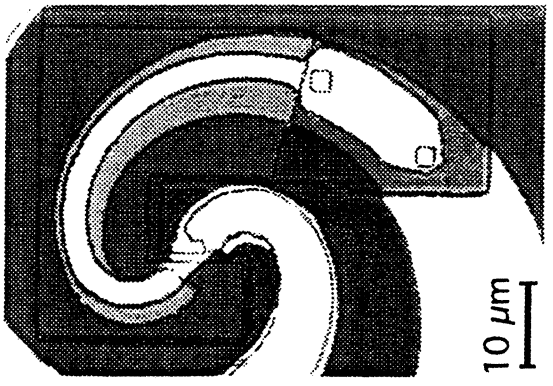

Figure 3 *Photo of the 500 GHz mixer chip. SIS junctions and the tuning circuit located at the apex of the spiral antenna. The two squares in the upper right part of the figure are the 2 μm × 2 μm area SIS junctions. The equivalent circuit diagram is shown in figure 4.*

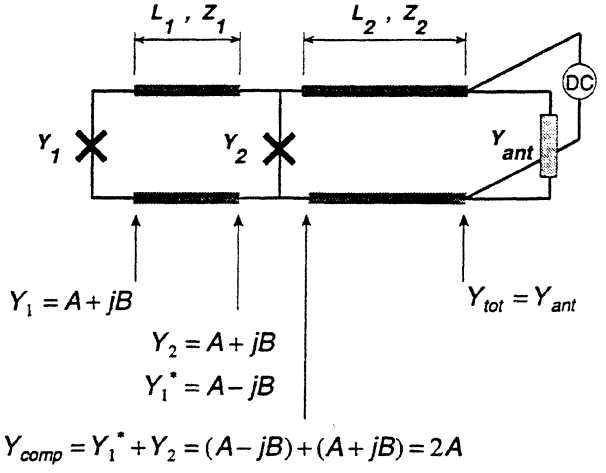

Figure 4 *Principle of the twin junction tuning circuit. The SIS junctions (represented by the admittances Y_1 and Y_2) are connected via a short transmission line with impedance Z_1. The length, L_1 , of this transmission line is such that the conjugate of Y_1 is obtained at the position of the second SIS junction. Then, the resulting real admittance is matched to the antenna admittance by a second transmission line, with impedance Z_2 and length L_2. Both junctions are DC-biased in parallel.*

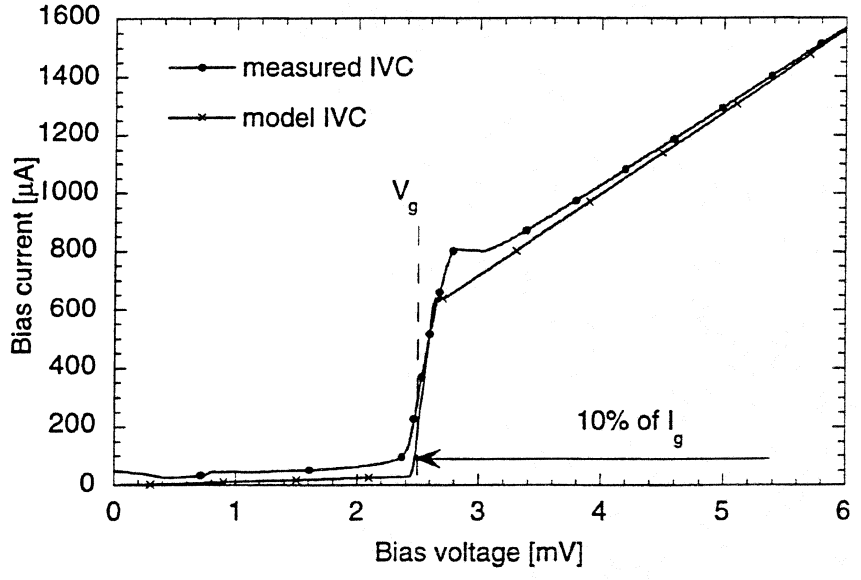

Figure 5 *Model IV curve approximation of real measured IVC. Gap voltage defines as the bias voltage at 10% current onset for evaluation of Nb material parameters.*

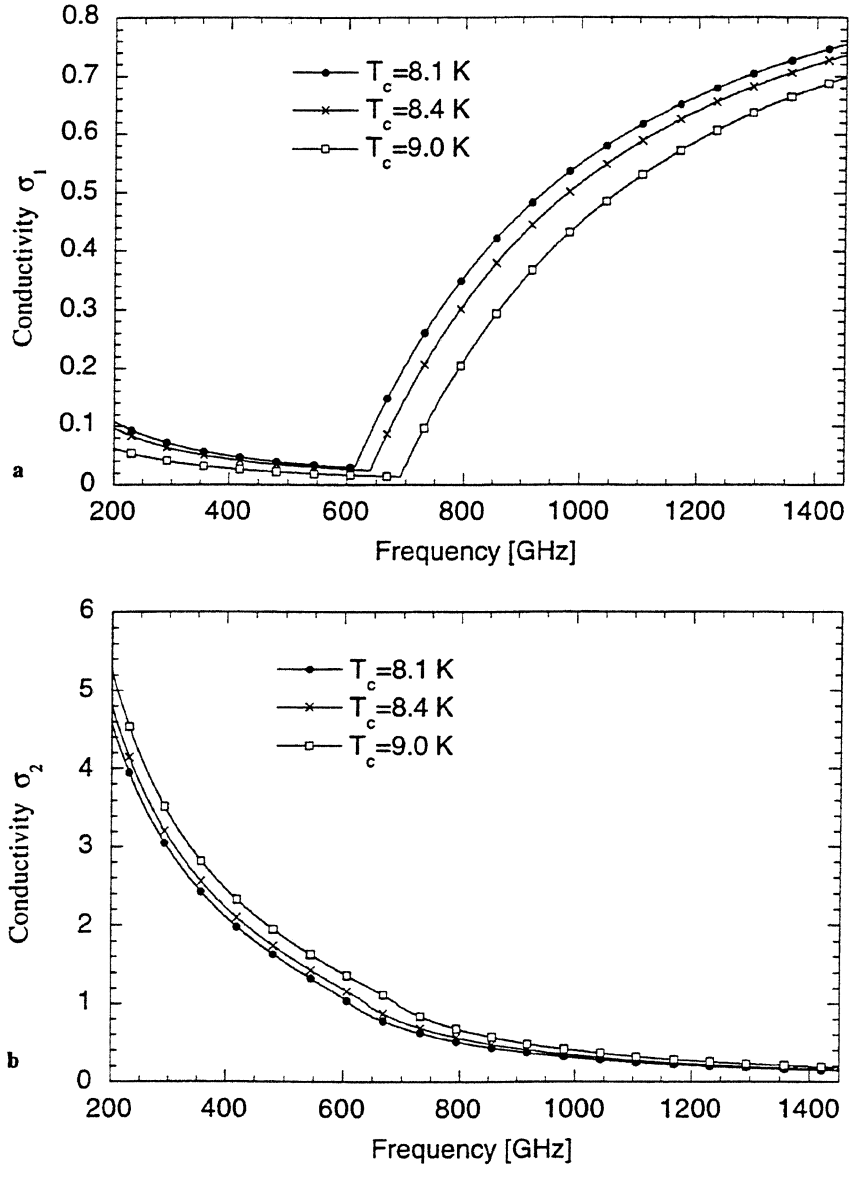

Figure 6 a,b *Calculated real and imaginary components σ_1, σ_2 for the Nb films presented in Table 3 vs. frequency .*

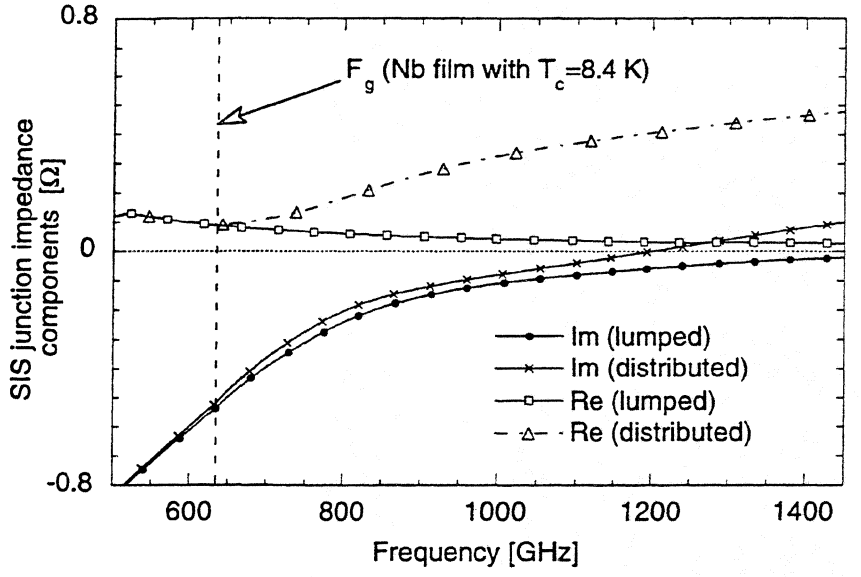

Figure 7 *Modeling of SIS junction as distributed and lump circuit (R//C). Plotted results for SIS junction of 2 μm (width) and 1.5 μm (length), R_n=6.7 Ω. Here Nb material was assumed to have T_c=8.4 K (see Table 3). U_{bias} was set at the middle of the first quasiparticle step with LO power level to be α=0.97*

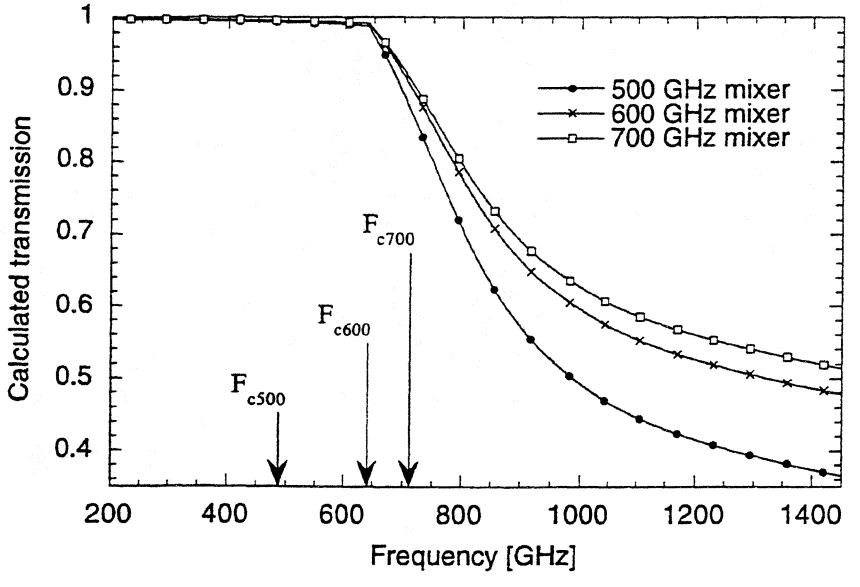

Figure 8 *Calculated transmission of the transformer sections for the studied mixers; here Nb material was assumed to have T_c=8.4 K (see Table 3), ambient temperature set to 4.2 K. Arrows indicate center of the tuning bands, where the transformers have quarter—wave lengths.*

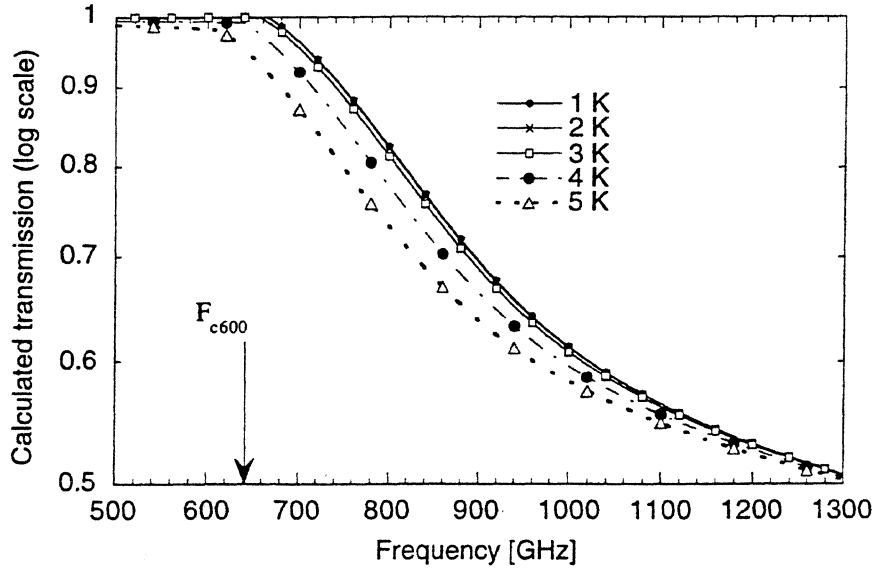

Figure 9 *Calculated transmission of the transformer section for the 600 GHz mixer; Nb material was assumed to have T_c=8.4 K (see Table 3), plotted for ambient temperatures 1-5 K. The arrow indicates center of the tuning band, where the transformer has quarter—wave length.*

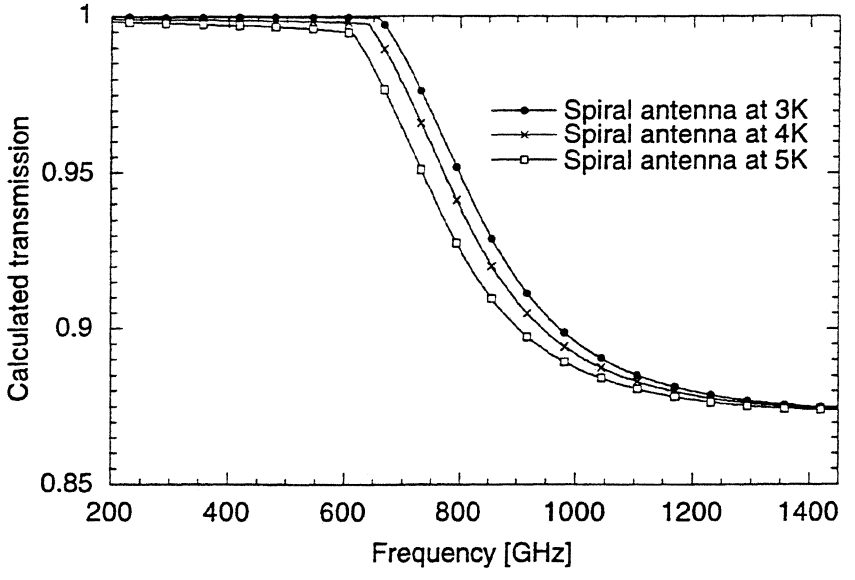

Figure 10 *Transmission of the equivalent line for the spiral antenna of 600/700 GHz mixers (inner radii 7 μm and outer radii 315 μm) at different ambient temperatures. The equivalent line current length in modeling corresponds to the active area of antenna 0.4λ in diameter.*

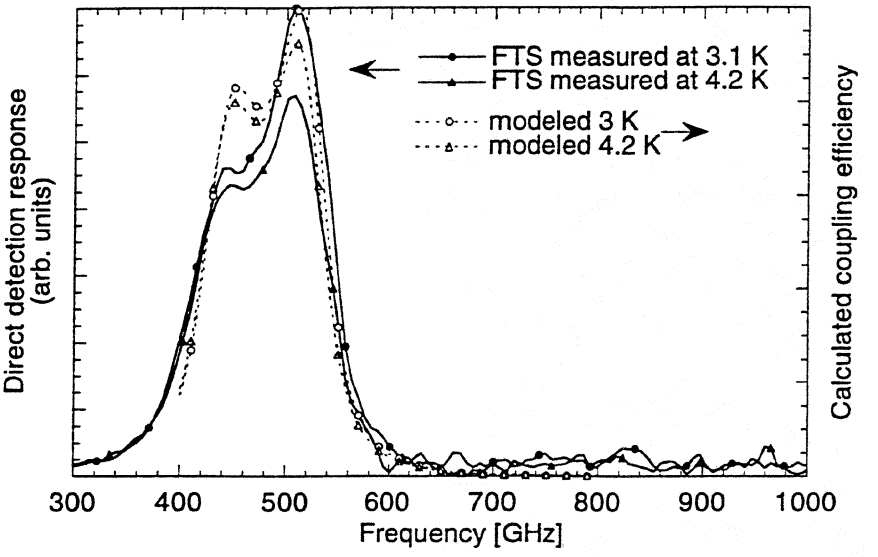

Figure 11 *The 500 GHz mixer: FTS measured direct detector responses and modeled coupling efficiencies at different ambient temperatures, i.e. 3 K and 4.2 K. Modeling was done for the measured sample parameters R_n, V_g, T_c=8.4 K, etc.*

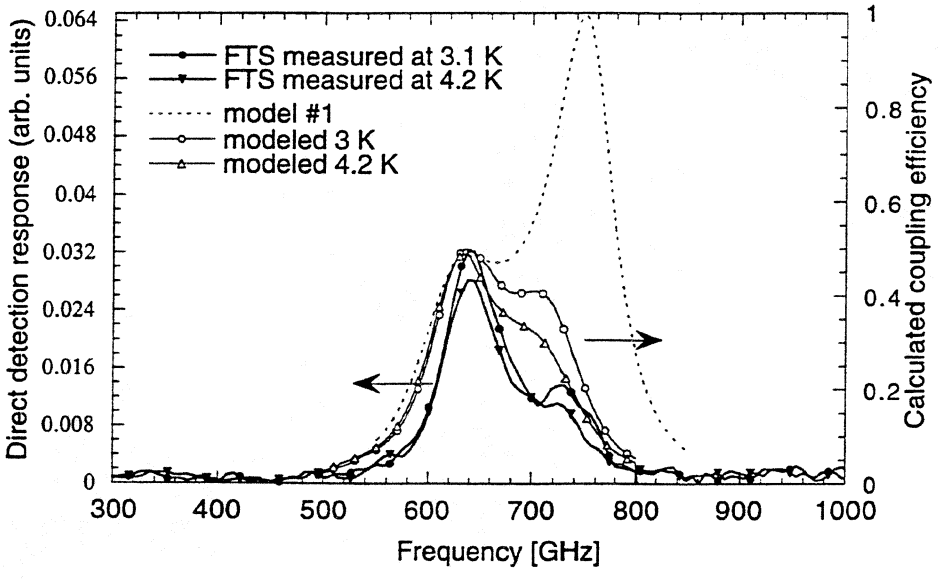

Figure 12 *The 600 GHz mixer (real circuit measured to be tuned to higher frequency than presented in Figure 1 because of improper SiO insulator thickness in conjugator): FTS measured direct detector responses and modeled coupling efficiencies are presented. Model #1 is the result of modeling for loss-free tuning circuitry, other curves at different ambient temperatures, i.e. 3 K and 4.2 K are for model including loss. Modeling was done for the measured sample parameters R_n, V_g, T_c=8.4 K, etc.*

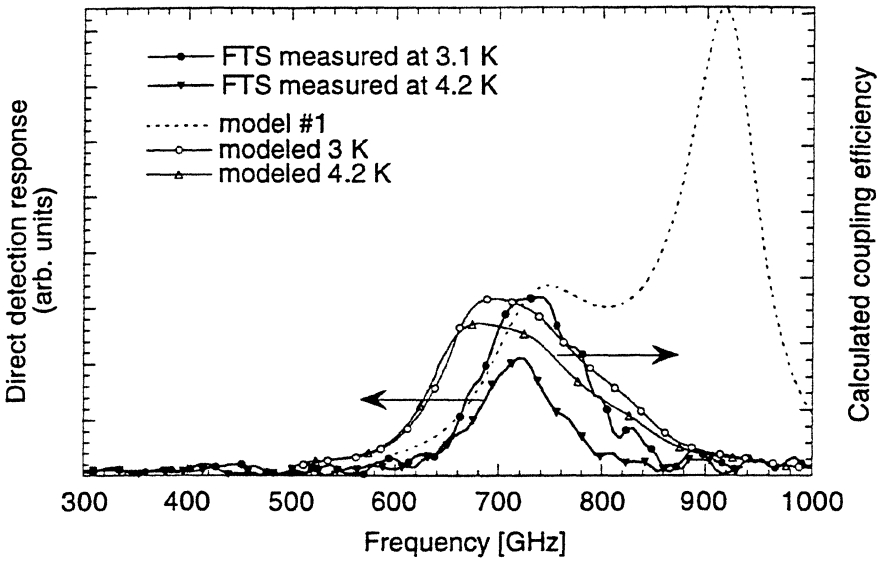

Figure 13 *The 700 GHz mixer (real circuit measured to be tuned to higher frequency than that presented in Figure 1 because of improper SiO insulator thickness in conjugator): FTS measured direct detector responses and modeled coupling efficiencies are presented. Model #1 curve is the result of modeling for loss-free tuning circuitry, other curves at different ambient temperatures, i.e. 3 K and 4.2 K are for model including loss. Modeling was done for the measured sample parameters R_n, V_g, T_c=8.4 K, etc.*

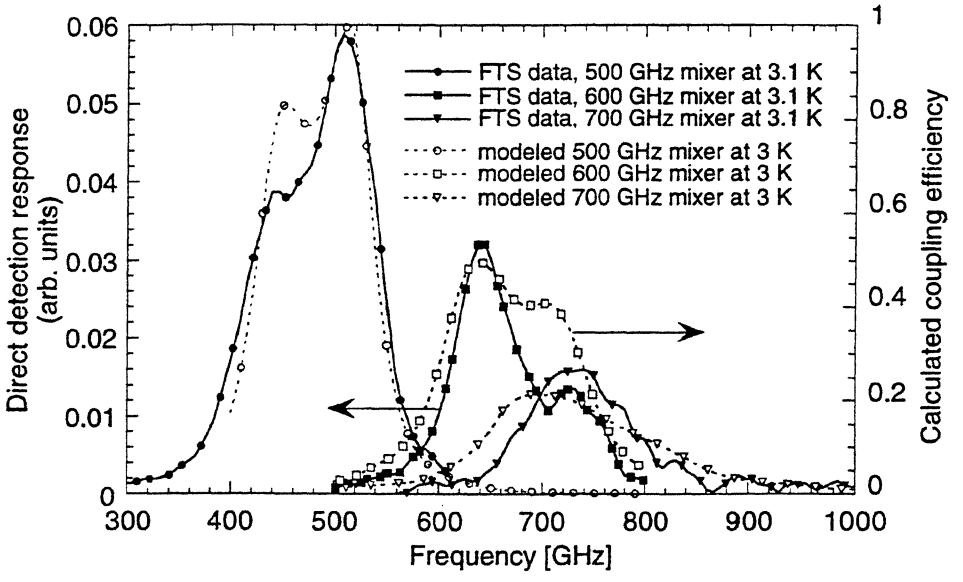

Figure 14 *The compiled data for 500, 600 and 700 GHz in original FTS measured scale and results of modeling. Accuracy of the tuning bands and coupling efficiencies is better or about 15% over the 400-1000 GHz band.*

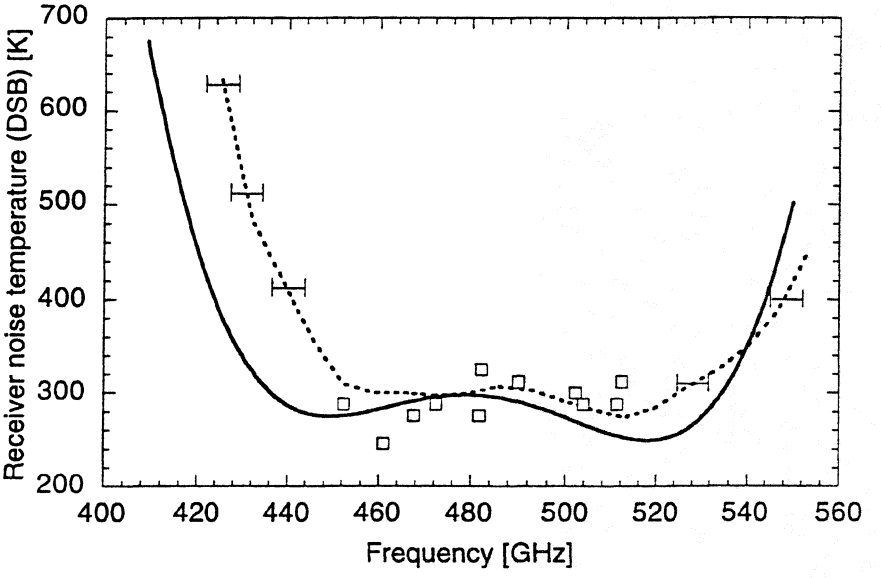

Figure 15 *The 500 GHz receiver measured noise temperatures (DSB) (❑). The dashed curve is FTS measured direct detector response for the same sample and the solid line is the result of modeling (coupling efficiency) for measured Rn, Vg, etc. The two latter curves are inverted and normalized to the measured receiver noise temperature at 480 GHz.*